THE JOURNAL OF BIOLOGICAL CHEMISTRY Vol. 278, No. 12, Issue of March 21, pp. 10182–10188, 2003
Printed in U.S.A.

Dependence of Purinergic P2X Receptor Activity on Ectodomain Structure*

Received for publication, September 5, 2002, and in revised form, January 7, 2003
Published, JBC Papers in Press, January 10, 2003, DOI 10.1074/jbc.M209094200

Mu-Lan He, Hana Zemkova, and Stanko S. Stojilkovic‡

From the Endocrinology and Reproduction Research Branch, NICHD, National Institutes of Health, Bethesda, Maryland 20892-4510

Purinergic receptors (P2XRs) activate and desensitize in response to the binding of extracellular nucleotides in a receptor- and ligand-specific manner, but the structural bases of their ligand preferences and channel kinetics have been incompletely characterized. Here we tested the hypothesis that affinity of agonists for binding domain accounts for a ligand-specific desensitization pattern. We generated chimeras using receptors with variable sensitivity to ATP in order: $P2X_4R$ > $P2X_{2a}R$ = $P2X_{2b}R$ ≫ $P2X_7R$. Chimeras having the ectodomain Ile^{66}–Tyr^{310} sequence of $P2X_2R$ and Val^{61}–Phe^{313} sequence of $P2X_7R$ in the backbone of $P2X_4R$ were expressed but were non-functioning channels. $P2X_{2a}$ + X_4R and $P2X_{2b}$ + X_4R chimeras having the Val^{66}–Tyr^{315} ectodomain sequence of $P2X_4R$ in the backbones of $P2X_{2a}R$ and $P2X_{2b}R$ were functional and exhibited increased sensitivity to ligands as compared with both parental receptors. These chimeras also desensitized faster than parental receptors and in a ligand-nonspecific manner. However, like parental $P2X_{2b}R$ and $P2X_{2a}R$, chimeric $P2X_{2b}$ + X_4R desensitized more rapidly than $P2X_{2a}$ + X_4R, and the rate of desensitization of $P2X_{2a}$+X_4R increased by substituting its Arg^{371}–Pro^{376} intracellular C-terminal sequence with the Glu^{376}–Gly^{381} sequence of $P2X_4R$. These results indicate the relevance of interaction between the ectodomain and flanking regions around the transmembrane domains on ligand potency and receptor activation. Furthermore, the ligand potency positively correlates with the rate of receptor desensitization but does not affect the C-terminal-specific pattern of desensitization.

Purinergic receptors (P2XRs)[1] are a family of ligand-gated receptor channels that open in response to the binding of extracellular ATP. Like other ligand-gated receptor channels, P2XRs also become refractory to the stimulus during the sustained agonist occupancy. This process, called desensitization, was initially characterized in acetylcholine receptors by Katz and Thesleff (1) and occurs because receptors enter stable desensitized states in which ion permeation is blocked or attenuated although ligand remains bound. Significant progress has been made recently in characterizing the ectodomain architecture of other ligand-gated receptor channels and the relationship between ligand-binding domain occupancy and receptor activity (2–4). However, the boundaries of the ectodomain and ATP-binding domain of P2XRs and the molecular mechanisms of transduction of information from ligand-binding domain to the pore of channels are largely unknown (5).

Modification at the triphosphate moiety of ATP served well in identification of native P2XR subtypes and provided useful information about the putative ligand-binding domain. For example, the substitution of bridging oxygen between α- and β-phosphorus with a methylene group resulted in a ligand, called αβ-meATP, which is a high potency agonist for $P2X_1R$ and $P2X_3R$, low potency agonist for $P2X_2R$, and partial agonist for $P2X_4R$ (6). High sensitivity of $P2X_3R$ to αβ-meATP can be transferred to $P2X_{2a}R$ and $P2X_{2b}R$ subtypes by generating the extracellular chimeras having the ectodomain of the $P2X_3$ subunit in the $P2X_2$-based backbone (7). These chimeras also exhibited enhanced rates of desensitization (7, 8). Within this region, single residue mutation studies have identified positively charged Lys^{68}, Lys^{70}, and Lys^{309} of $P2X_1R$ and the corresponding Lys^{69} and Lys^{71} of $P2X_2R$ as contributing to the ATP-binding site and control of rate of receptor desensitization (9, 10). In general agreement with these observations, the N-terminal half of the $P2X_3$ ectodomain, from Val^{60} to Arg^{180}, is necessary for high αβ-meATP sensitivity of the receptor. The attempt to further narrow this region was obstructed, indicating that the ectodomain is sensitive to modification by site-directed mutagenesis (7).

P2XRs activate and desensitize in a receptor- and ligand-specific manner. When stimulated with ATP, $P2X_1R$ and $P2X_3R$ desensitize very rapidly (in an ms time scale), $P2X_4R$ and $P2X_6R$ desensitize with a moderate rate (within a few seconds), and $P2X_2R$, $P2X_5R$, and $P2X_7R$ show little or no desensitization (11, 12). Two main hypotheses emerged from previous work on desensitization of P2XRs, one based on the structure of channels and the other based on the actions of intracellular messengers. Heteromultimerization results in P2XRs that desensitize with different kinetics from those seen in cells expressing homomeric receptors (13–15). The site-directed mutagenesis experiments indicated the relevance of C-terminal structure on the desensitization of P2XR (15–19), as well as the relevance of a highly conserved N-terminal site for protein kinase C in functional desensitization of receptors (19–21). Phosphorylation of a protein kinase A site in C-terminal of $P2X_{2a}R$ may also participate in receptor desensitization (22). In parallel to other ligand-gated receptor channels (2, 23–28), the ligand-binding domain of P2XRs may also contribute to the control of rates of desensitization (7, 8).

Here, we extended investigations on the relevance of the ectodomain structure on ligand selectivity and the pattern of P2XR desensitization. Experiments were done with wild-type

* The costs of publication of this article were defrayed in part by the payment of page charges. This article must therefore be hereby marked "*advertisement*" in accordance with 18 U.S.C. Section 1734 solely to indicate this fact.

‡ To whom correspondence should be addressed: SCS/ERRB/NICHD, Bldg. 49, Rm. 6A-36, 49 Convent Dr., Bethesda, MD 20892-4510. Tel.: 301-496-1638; Fax: 301-594-7031; E-mail: stankos@helix.nih.gov.

[1] The abbreviations used are: P2XRs, purinergic receptor channels; αβ-meATP, α,β-methylene-ATP; BzATP, 3′-O-(4-benzoyl)benzoyl-ATP; GFP, green fluorescent protein; EGFP, enhanced GFP; AMPA, α-amino-3-hydroxy-5-methyl-4-isoxazoleproprionic acid.

$P2X_{2a}R$, $P2X_{2b}R$, and $P2X_4R$ and chimeric $P2X_{2a} + X_4R$ and $P2X_{2b} + X_4R$ containing the ectodomain sequence of $P2X_4R$ instead of the corresponding $P2X_2R$ sequence. The reverse $P2X_4 + X_2R$ chimera was also constructed, as well as the $P2X_4 + X_7R$ chimera containing the ectodomain sequence of $P2X_7R$. To clarify the possible interaction between the ectodomain and C-terminal domain in control of agonist specificity and receptor activity, we also constructed $P2X_{2a\text{-}6aa} + X_4R$ mutant chimera containing the C-terminal 6-residue sequence of $P2X_4R$ instead of the corresponding sequence of $P2X_{2a} + X_4R$. Both whole-cell patch clamp current recordings and calcium measurements were used to estimate the activity of receptors in response to ATP, the native agonist for P2XRs, and two agonist analogs, BzATP and $\alpha\beta$-meATP. The results of these investigations clearly indicate the C-terminal-independent influence of the ectodomain structure on agonist potency and rate of P2XR desensitization.

MATERIALS AND METHODS

DNA Constructs, Cell Culture, and Transfection—The coding sequences of the rat $P2X_{2a}$, $P2X_{2b}$, $P2X_4$ subunits were isolated by reverse transcription-PCR (15) and subcloned into the biscistronic enhanced fluorescent protein expression vector, pIRES2-EGFP (Clontech), at the restriction enzyme sites of *Xho*I/*Pst*I for $P2X_{2a}R$ and $P2X_{2b}R$ and *Xho*I/*EcoR*I for $P2X_4R$. Chimera $P2X_{2a} + X_4R$, $P2X_{2b} + X_4R$, $P2X_4 + X_2R$, and $P2X_4 + X_7R$ were directly constructed by overlap extension PCR using the corresponding wild-type P2XRs cDNA as templates. Mutagenesis primers were pairs of chimeric sense and antisense that were 36-mer long with the joint sites positioned at the center. The constructed $P2X_{2a} + X_4R$, $P2X_{2b} + X_4R$ chimeric subunits replace Ile^{66}–Tyr^{310} with Val^{66}–Tyr^{315} extracellular domain of $P2X_4R$, whereas $P2X_4 + X_2R$ and $P2X_4 + X_7R$ contain the Ile^{66}–Tyr^{310} and Val^{61}–Phe^{313} sequence of $P2X_2R$ and $P2X_7R$, respectively, instead of the native Val^{66}–Tyr^{315} of $P2X_4R$. We also constructed a mutant of chimera $P2X_{2a} + X_4R$, termed $P2X_{2a\text{-}6aa} + X_4R$, by overlap extension PCR, as described previously (15). This mutant contains the Glu^{376}–Gly^{381} sequence of $P2X_4R$ instead of the corresponding Arg^{371}–Pro^{376} sequence of $P2X_{2a} + X_4R$. These chimeric P2XRs were subcloned into GFP expression vector pIRES2-EGFP. The identity of all constructs was verified by dye terminator cycle sequencing (PerkinElmer Life Sciences), performed by the Laboratory of Molecular Technology (NCI, National Institutes of Health, Frederick, MD). The large scale plasmid DNAs for transfection were prepared using a Qiagen Plasmid Maxi kit (Qiagen).

Mouse immortalized gonadotropin-releasing hormone-secreting cells (hereafter GT1 cells) and human embryonic kidney cells (hereafter HEK293 cells) were used in functional studies of wild-type and mutant P2XRs, as described previously (15). GT1 cells were routinely maintained in Dulbecco's modified Eagle's medium/Ham's F12 medium (1:1) containing 10% (v/v) fetal bovine serum and 100 μg/ml gentamicin (Invitrogen) in a water-saturated atmosphere of 5% CO_2 and 95% air at 37 °C. HEK293 cells were cultured in minimum Eagle's medium supplemented with 10% horse serum and 100 μg/ml gentamicin. Before the day of transfection, cells were plated on 25-mm poly-L-lysine (0.01% w/v; Sigma)-coated coverslips at a density of $0.75–1 \times 10^5$ cells/35-mm dish. For each dish of cells, transient transfection of expression constructs was conducted using 1 μg of DNA and 7 μl of LipofectAMINE 2000 reagent (Invitrogen) in 3 ml of serum-free Opti-MEM. After 6 h of incubation, the transfection mixture was replaced with normal culture medium. Cells were subjected to experiments 24–48 h after transfection.

Calcium Measurements—Transfected GT1 cells were preloaded with 1 μM Fura-2 acetoxymethyl ester (Fura-2/AM; Molecular Probes, Eugene, OR) for 60 min at room temperature in modified Krebs-Ringer buffer: 120 mM NaCl, 5 mM KCl, 1.2 mM $CaCl_2$, 0.7 mM $MgSO_4$, and 15 mM HEPES plus 1.8 g/liter glucose (pH 7.4). After dye loading, cells were incubated in Modified Krebs-Ringer buffer and kept in the dark for at least 30 min before single-cell $[Ca^{2+}]_i$ measurements. Coverslips with cells were mounted on the stage of an Axiovert 135 microscope (Carl Zeiss, Oberkochen, Germany) attached to the Attofluor digital fluorescence microscopy system (Atto Instruments, Rockville, MD). Cells were stimulated with various doses of agonists, the dynamic changes of $[Ca^{2+}]_i$ were examined under a ×40 oil immersion objective during exposure to alternating 340- and 380-nm light beams, and the intensity of light emission at 520 nm was measured. The ratio of light intensities, F_{340}/F_{380}, which reflects changes in $[Ca^{2+}]_i$, was simultaneously followed in several single cells. GFP was used as a marker for cells with P2XR expression as described previously (15). Cells expressing GFP were optically detected by an emission signal at 520 nm when excited by a 488-nm ultraviolet light. Experiments were done in cells with comparable GFP fluorescence signals (about 60 arbitrary units), and no repetitive stimulation was done to avoid the possible impact of desensitization on the amplitude and pattern of $[Ca^{2+}]_i$ signals.

Current Measurements—Electrophysiological experiments were performed on HEK293 cells at room temperature using whole-cell patch clamp recording techniques (29). ATP-induced currents were recorded using an Axopatch 200B patch clamp amplifier (Axon Instruments, Union City, CA) and were filtered at 2 kHz using a low pass Bessel filter. 40–70% series resistance compensation was used. Patch electrodes, fabricated from borosilicate glass (type 1B150F-3; World Precision Instruments, Sarasota, FL) using a Flaming Brown horizontal puller (P-87; Sutter Instruments, Novato, CA), were heat-polished to a final tip resistance of 3–5 megaohms. All current records were captured and stored using the pClamp 8 software packages in conjunction with the Digidata 1322A A/D converter (Axon Instruments). Patch electrodes were filled with a solution containing 140 mM KCl, 0.5 mM $CaCl_2$, 1 mM $MgCl_2$, 5 mM EGTA, and 10 mM HEPES; the pH was adjusted with 1 M KOH to 7.2. The osmolarity of the internal solutions was 282–287 mosM. The bath solution contained 142 mM NaCl, 3 mM KCl, 1 mM $MgCl_2$, 2 mM $CaCl_2$, 10 mM glucose, and 10 mM HEPES; the pH was adjusted to 7.3 with 1 M NaOH. The osmolarity of this solution was 285–295 mosM. A 3 M KCl agar bridge was placed between the bathing solution and the reference electrode. ATP was applied for 60 s using a fast gravity-driven microperfusion system (BPS-8, ALA Scientific Instruments, Westbury, NY). The application tip was routinely positioned about 500 μm above the recorded cell. Less than 600 ms was required for complete exchange of solutions around the patched cells, as estimated from altered potassium current (10–90% rise time). The time between each ATP application was about 10 min to allow recovery from receptor desensitization.

Calculations—The time course of the $[Ca^{2+}]_i$ was fitted to a single exponential function (ae^{-ktb+b}) using GraphPad Prism (GraphPad Software, San Diego, CA) to generate the rates of signaling desensitization (k) and half-times of decay ($\tau = ln2/k$). The time courses of currents evoked by sustained ATP stimulation were fitted to a single exponential function using the pClamp 8 program (Axon Instruments). Significant differences, with $p < 0.05$, were determined by one-way analysis of variance with Newman-Keuls multiple comparison test. Concentration-response relationships were fitted to a four-parameter logistic equation using a non-linear curve-fitting program, which derives 50% efficient concentrations (EC_{50}) and 50% desensitizing concentrations (DC_{50}) (Kaleidagraph, Synergy Software, Reading, PA).

RESULTS

Characterization of Wild-type and Chimeric P2XRs—When expressed in GT1 cells under identical experimental conditions, parental receptors $P2X_{2a}R$, $P2X_{2b}R$, and $P2X_4R$ responded to ATP, BzATP, and $\alpha\beta$-meATP stimulation with a rapid rise in $[Ca^{2+}]_i$ followed by a gradual decline toward steady plateau levels. In accordance with previously published data (8, 30), in all agonist concentrations studied, the peak $[Ca^{2+}]_i$ responses were comparable in $P2X_{2a}R$- and $P2X_{2b}R$-expressing cells. Fig. 1*A* illustrates the concentration dependence of three agonists on the peak amplitude of $[Ca^{2+}]_i$ responses for both receptor subtypes combined. The calculated EC_{50} values (Fig. 1, *dotted vertical lines*) were in general agreement with the data in the literature (6): ATP was the most potent agonist for $P2X_2Rs$, followed by BzATP, whereas $\alpha\beta$-meATP acted as a low potency agonist.

On the other hand, the estimated EC_{50} values for ATP, BzATP, and $\alpha\beta$-meATP in GT1 cells expressing rat $P2X_4R$ (Fig. 1*B*) differed significantly from previously published data (reviewed in Ref. 6). In our experiments, ATP was a highly potent agonist for these receptors, with an EC_{50} of about 1 μM, and the calculated EC_{50} for BzATP was 2.5 μM as compared with >500 μM reported in other expression systems. At supramaximal concentrations, the peak amplitudes of ATP- and BzATP-induced $[Ca^{2+}]_i$ responses in $P2X_4R$-expressing cells were about 40% of those observed in $P2X_2R$-expressing cells, whereas the peak amplitudes of current responses were comparable (Fig. 1).

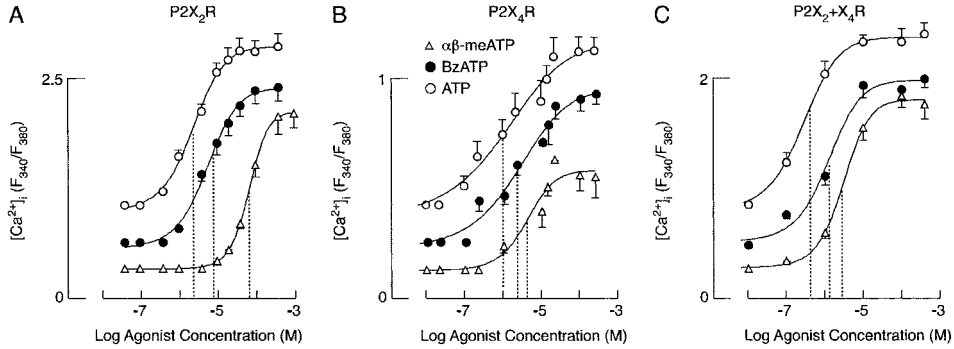

FIG. 1. **Concentration-dependent effects of agonists on peak calcium response in single cells expressing homomeric P2XRs.** *A–C*, comparison of the effects of ATP and its two analogs, BzATP and $\alpha\beta$-meATP, on peak calcium response in cells expressing $P2X_{2a}R$ and $P2X_{2b}R$ (*A*), $P2X_4R$ (*B*), and $P2X_{2a} + X_4R$ and $P2X_{2b} + X_4R$ (*C*). Data shown are means ± S.E. derived from 3 to 11 experiments per dose, each done in at least 15 single cells. The results for $P2X_{2a}R$ and $P2X_{2b}R$ (*A*) and $P2X_{2a} + X_4R$ and $P2X_{2b} + X_4R$ (*C*) are combined because no differences in peak $[Ca^{2+}]_i$ responses were observed between them. *Dotted vertical lines* indicate the calculated EC_{50} values for three agonists. $P2X_2 + X_4R$ chimeras were constructed as described under "Materials and Methods."

$\alpha\beta$-meATP-induced peak current/$[Ca^{2+}]_i$ responses were 44% as compared with those in ATP- and BzATP-stimulated cells, consistent with the partial agonist action of this ATP analog observed in other expression systems (31), but the calculated EC_{50} was 4 μM (Fig. 1*B*).

The $P2X_{2a} + X_4R$ and $P2X_{2b} + X_4R$ chimeras having the ectodomain of $P2X_4R$ in the backbone of $P2X_{2a}R$ and $P2X_{2b}R$, respectively, were functional and responded to three agonists in a concentration-dependent manner with highly comparable peak amplitudes. Fig. 1*C* illustrates the combined results for both receptors. Chimeric receptors differed from parental receptors in two respects. First, although the structure of the pore was not altered, the peak amplitudes of $[Ca^{2+}]_i$ responses in chimeric receptors were 80% of those observed in $P2X_{2a}R$- and $P2X_{2b}R$-expressing cells ($p < 0.01$ in the 10–1000 μM concentration range of ATP). Second, chimeric receptors exhibited higher sensitivity to ATP as compared with both parental receptors, and $\alpha\beta$-meATP exhibited the full agonistic action as compared with partial agonistic action in $P2X_4R$- expressing cells.

The reverse $P2X_4 + X_2R$ chimera, having the ectodomain of $P2X_2R$ inserted into the backbone of $P2X_4R$, was expressed at the levels comparable with those observed in experiments with $P2X_{2a} + X_4R$ and $P2X_{2b} + X_4R$, as estimated by GFP fluorescence intensity. However, the receptor did not respond to ATP in the 1–1000 μM concentration range. The lack of effects of ATP was not due to the endogenous desensitization of receptors because ATP was also ineffective in cells cultured in the presence of apyrase, an ectoATPase. Also, the $P2X_4 + X_7R$ chimera having the ectodomain of $P2X_7R$ instead of $P2X_4R$ was expressed but was not functional in the presence or absence of apyrase. All together, experiments with chimeras suggested that although the ectodomain sequences we selected contained several residues critical for ligand binding, they were not sufficient to preserve intact ligand-binding domains. The $P2X_4R$-specific ligand potency was enhanced, whereas the $P2X_2R$- and $P2X_7R$-specific ligand potency was abolished in chimeric channels, indicating the interaction between the ectodomain and nearby residues.

Receptor-specific Desensitization Pattern—To characterize the pattern of receptor desensitization and its impact on calcium signaling, both current and calcium measurements were used. Fig. 2*A* illustrates typical profiles of ATP (100 μM)-induced current responses in cells expressing wild-type $P2X_{2a}R$, $P2X_{2b}R$, and $P2X_4R$. The peak amplitudes of current responses were in high pA ($P2X_4R$) to low nA ($P2X_{2a}R$ and $P2X_{2b}R$) range. Consistent with previously published data (16), $P2X_{2a}R$ desensitized slowly and incompletely, reaching the steady levels with

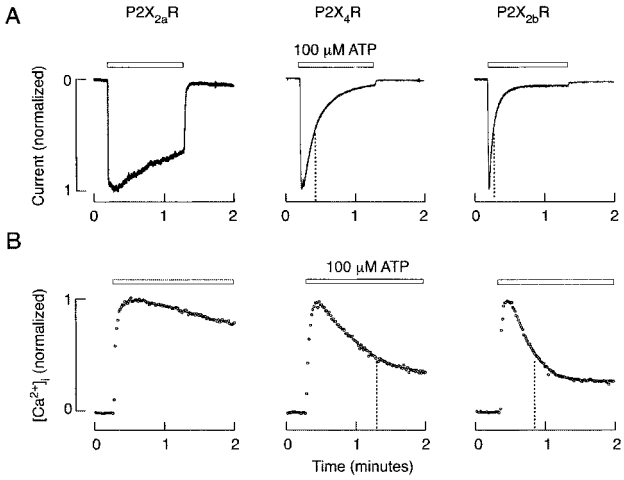

FIG. 2. **Receptor-specific desensitization pattern of P2XRs.** *A* and *B*, comparison of the effects of ATP on the pattern of current (*A*) and calcium (*B*) responses in cells expressing wild-type $P2X_{2a}R$ (*left traces*), $P2X_4R$ (*central traces*), and $P2X_{2b}R$ (*right traces*). In this and following figures, experimental records for current responses are shown by *solid lines* and are representative from at least 20 traces per receptor, whereas experimental records for calcium response are shown by *open circles* (mean values from at least 15 traces in representative experiments). *Horizontal bars* indicate the time of exposure to 100 μM ATP. The current traces shown are from cells clamped at −50 mV.

a τ of 22 s, whereas $P2X_{2b}R$ desensitized rapidly with a calculated τ of about 4 s. $P2X_4R$ desensitized to the steady levels comparable with $P2X_{2b}R$ but with a τ of about 9 s.

The significance of receptor-specific desensitization pattern on $[Ca^{2+}]_i$ response is illustrated in Fig. 2*B*. Three receptors generated calcium signals, which differed in profiles. The rates of signal desensitization (expressed as τ) were: 96 s in $P2X_{2a}R$-expressing cells, 18 s in $P2X_{2b}R$-expressing cells, and 45 s in $P2X_4R$-expressing cells. Differences in the calculated τ values in current and $[Ca^{2+}]_i$ measurements illustrate the impact of calcium-handling mechanisms of the cells used in experiments on the rate of receptor desensitization. On the other hand, the relative ratios in the rates of $P2X_{2a}R$, $P2X_{2b}R$, and $P2X_4R$ desensitization estimated from two measurements were highly comparable. This clearly indicates that $[Ca^{2+}]_i$ measurements not only provide information about the physiological relevance of receptor activation and desensitization but also could be used as valuable parameters in characterizing the nature of P2XR desensitization, at least for slower desensitizing receptors.

A comparison between the patterns of current responses in

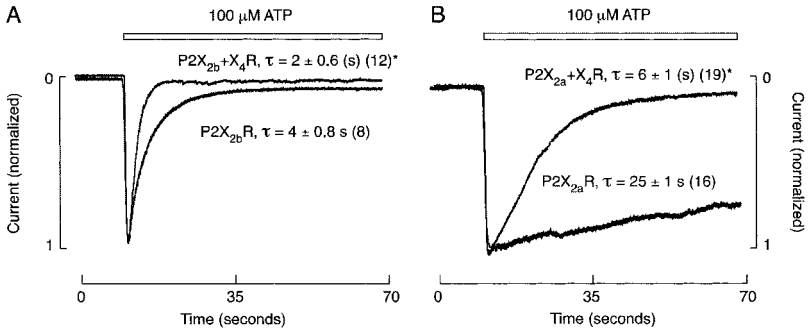

FIG. 3. **Acceleration of $P2X_{2a}R$ and $P2X_{2b}R$ desensitization by substituting their common ectodomain with the $P2X_4R$ ectodomain (current recordings).** The traces shown are representative for wild-type $P2X_{2b}R$ and chimeric $P2X_{2b}$ + X_4R (A) and wild-type $P2X_{2a}R$ and chimeric $P2X_{2a}$ + X_4R (B). The mean ± S.E. values are shown *above* traces, and the *numbers* in *parentheses* indicate the number of records for each receptor. *Asterisks* indicate significant differences ($p < 0.05$) between the pairs.

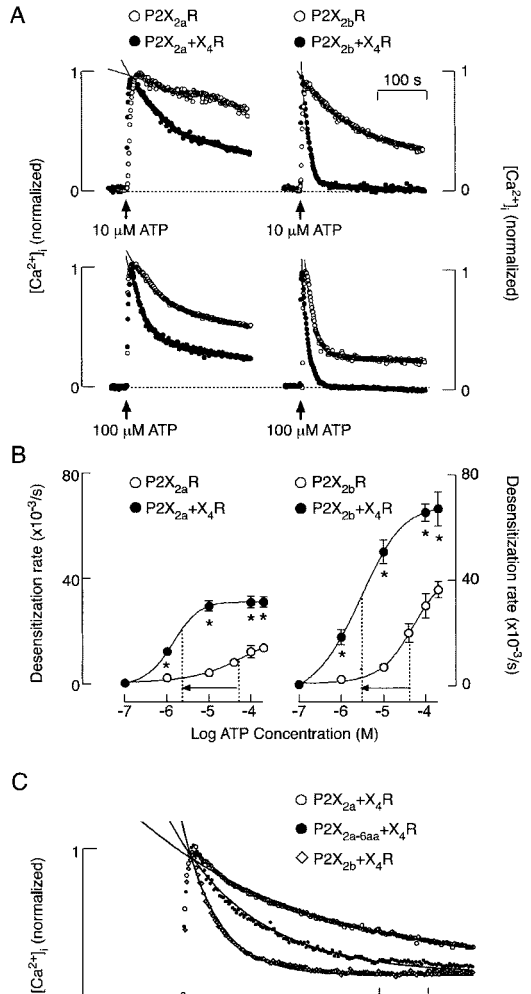

FIG. 4. **Influence of ectodomain and C-terminal domain on acceleration of $P2X_{2a}$ + X_4R and $P2X_{2b}$ + X_4R desensitization (calcium recordings).** *A*, representative traces of calcium responses in cells stimulated with 10 μM ATP (*upper traces*) and 100 μM ATP (*bottom traces*). In this and following figures, experimental records are shown by *open circles* (mean values from at least 15 traces in representative experiments), and fitted curves are shown by *full lines*. A single exponential function was sufficient to describe the desensitization rates. The fitted function is extrapolated for clarity. *B*, concentration dependence of ATP on the rate of P2XR desensitization. *Asterisks* indicate significant differences ($p < 0.01$) between the pairs. *Vertical dotted lines* indicate the calculated DC_{50} values, and *horizontal arrows* indicate a leftward shift in DC_{50} values for chimeric channels. *C*, comparison of 100 μM ATP-induced $[Ca^{2+}]_i$ signals in GT1 cells expressing $P2X_{2a}$ + X_4R, $P2X_{2a\text{-}6aa}$ + X_4R, and $P2X_{2b}$ + X_4R.

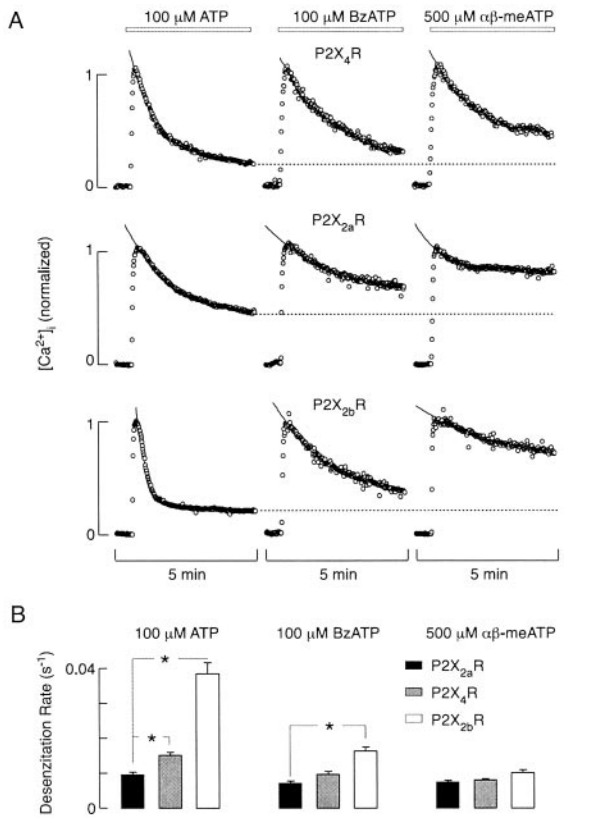

FIG. 5. **Ligand-specific receptor desensitization pattern of wild-type P2XRs.** *A*, representative traces of $[Ca^{2+}]_i$ response in cells expressing $P2X_4R$ (*upper traces*), $P2X_{2a}R$ (*central traces*), and $P2X_{2b}R$ (*bottom traces*). Traces shown are representative from 3–5 independent experiments. *Horizontal dotted lines* indicate differences in the plateau $[Ca^{2+}]_i$. *B*, mean values of rates of receptor desensitization. *Asterisks* indicate significant differences ($p < 0.01$) between the pairs.

cells expressing wild-type $P2X_{2a}R$ and $P2X_{2b}R$ and chimeric receptors is shown in Fig. 3. The substitution of the native $P2X_{2a}R$ ectodomain with $P2X_4$ ectodomain dramatically enhanced the rate of receptor desensitization (Fig. 3*B*). Significant differences were also observed between $P2X_{2b}R$ and $P2X_{2b}$ + X_4R (Fig. 3*A*). Both chimeric receptors also desensitized more rapidly than $P2X_4R$ (Fig. 3 *versus* Fig. 2). The same conclusion was reached in experiments with single cell calcium measurements. As shown in Fig. 4*A*, calcium signals desensitized more rapidly in cells expressing chimeric receptors when stimulated with 10 μM ATP (*upper panels*) and 100 μM ATP (*lower panels*). In parallel with changes in the EC_{50} values for chimeric receptors (Fig. 1), calcium signals also desensitized with about one log unit leftward shift in the DC_{50} values as compared with parental $P2X_2Rs$ (Fig. 4*B*). The ratios between τ values for current and calcium measurements in cells expressing two chimeric receptors were comparable with those observed in parental receptors. These results clearly indicate the relevance of the ectodomain structure on the kinetics of receptor desensitization and suggest that the ligand potency

TABLE I
The level of $[Ca^{2+}]_i$ signal desensitization in cells expressing parental and chimeric P2XRs

Agonist	Desensitization level (%)			
	$P2X_{2a}R$	$P2X_{2b}R$	$P2X_{2a} + X_4R$	$P2X_{2b} + X_4R$
ATP, 100 μM	59.9 ± 2.2	82.1 ± 1.0[a]	85.1 ± 2.7	100 ± 5.2[a]
BzATP, 100 μM	44.3 ± 11.4	72.0 ± 1.8[a]	76.7 ± 1.9	100 ± 2.4[a]
$\alpha\beta$-meATP, 500 μM	45.8 ± 3.2	43.4 ± 2.5	85.5 ± 2.2	97.8 ± 0.5[a]

[a] $p < 0.05$ vs. $P2X_{2a}R$ (second and third columns) and $P2X_{2a} + X_4R$ (fourth and fifth columns). Basal $[Ca^{2+}]_i$ was expressed as 0% and peak $[Ca^{2+}]_i$ response as 100%.

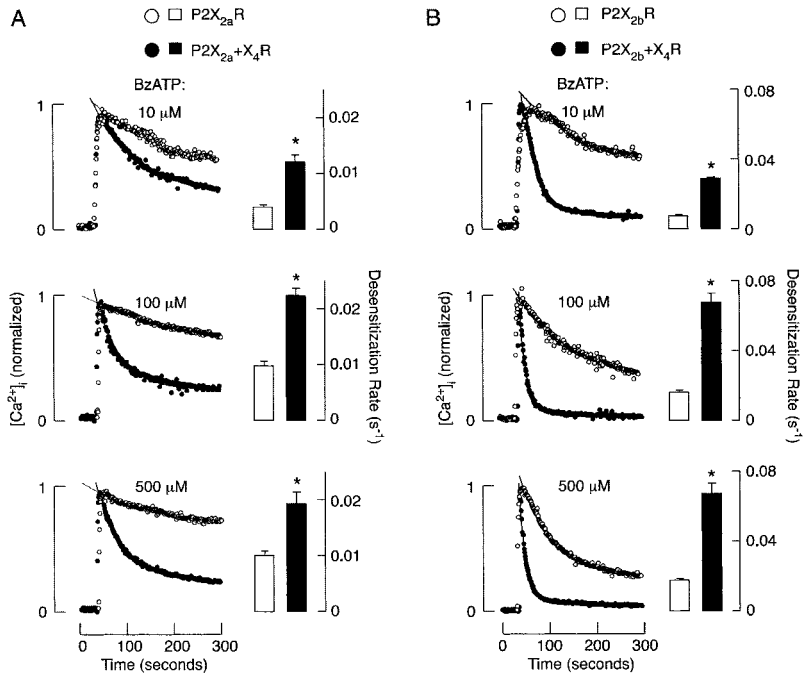

FIG. 6. **Comparison of BzATP-induced calcium signals in cells expressing wild-type and chimeric receptors.** *A*, concentration-dependent effects of BzATP on the pattern of calcium response in $P2X_{2a}R$ and $P2X_{2a} + X_4R$-expressing cells (*A*) and $P2X_{2b}R$ and $P2X_{2b} + X_4R$-expressing cells (*B*). In *A* and *B*, *left panels* illustrate representative traces, and *right panels* (*bars*) illustrate differences in the rates of calcium signal desensitization.

reflects on rate of receptor desensitization.

Current and calcium measurements showed that $P2X_{2b}+X_4R$ desensitized more rapidly than $P2X_{2a}+X_4R$, consistent with the hypothesis that the C-terminal-specific desensitization pattern was preserved in chimeric channels. To test this hypothesis further, we generated $P2X_{2a\text{-}6aa}+X_4R$ mutant chimera, having the Glu^{376}–Gly^{381} C-terminal sequence of $P2X_4R$ instead of the Arg^{371}–Pro^{376} sequence of $P2X_{2a}+X_4R$. Our earlier studies have shown the relevance of Arg^{371}–Pro^{376} in slowing the rate of receptor desensitization (16). Substitution of this sequence with the Glu^{376}–Gly^{381} sequence of $P2X_4R$ increased the rate of $P2X_{2a}R$ desensitization (15). In accordance with these observations, $P2X_{2a\text{-}6aa} + X_4R$ mutant chimera showed an increased rate of desensitization as compared with $P2X_{2a} + X_4R$ chimera (Fig. 4*C*), and the ratio between the rates of $P2X_{2a} + X_4R$, $P2X_{2a\text{-}6aa} + X_4R$, and $P2X_{2b} + X_4R$ was comparable with that observed in cells expressing $P2X_{2a}R$, $P2X_{2a\text{-}6aa}R$, and $P2X_{2b}R$ (15). Thus, the increase in the potency of receptors for ATP increases the rates of receptor desensitization independently of the C-terminal-controlled desensitization.

Ligand-specific Desensitization Pattern—In further experiments, we compared the patterns of calcium signals and rates of desensitization in response to ATP, BzATP, and $\alpha\beta$-meATP. Fig. 5 illustrates typical profiles of calcium signals in response to these three agonists in cells expressing parental receptors. In accordance with our previous study (8), the C-terminal-specific desensitization pattern of wild-type $P2X_2Rs$ observed in response to ATP (Fig. 5*A*, *left traces*) was partially mimicked by BzATP (*central traces*) but was lost in cells stimulated with $\alpha\beta$-meATP (*right traces*). The ligand specificity of receptor desensitization was also observed in cells expressing wild-type $P2X_4R$ (Fig. 5*A*, *upper traces*). The mean values of the rate of receptor desensitization in response to three agonists are shown in Fig. 5*B*. When stimulated with ATP, three receptors desensitized with significantly different rates (*left panel*). No differences in the rates of $P2X_{2a}R$ and $P2X_4R$ desensitization were observed in response to BzATP stimulation (*central panel*), and all three receptors desensitized with highly comparable kinetics when stimulated with $\alpha\beta$-meATP (*right panel*). The plateau $[Ca^{2+}]_i$ levels in response to three agonists also differed (illustrated by *dotted lines* in Fig. 5*A* and quantified in Table I).

In further studies, we examined the ligand-specific desensitization pattern of chimeric receptors. Fig. 6 compares typical calcium signal profiles in cells expressing wild-type $P2X_{2a}R$ and chimeric $P2X_{2a} + X_4R$ (Fig. 6*A*) and wild-type $P2X_{2b}R$ and chimeric $P2X_{2b} + X_4R$ (Fig. 6*B*) during the prolonged stimulation with increasing BzATP concentrations. The C-terminal-specific desensitization patterns of $P2X_{2a}R$ and $P2X_{2b}R$ that are present in ATP-stimulated cells (Fig. 5), but are lost in BzATP-stimulated cells (Figs. 5 and 6), were reestablished in BzATP-stimulated cells expressing chimeric receptors. Fig. 6*A* (*left panels*) shows a typical pattern of receptor desensitization in wild-type and chimeric $P2X_2Rs$, and bars (*right panels*) illustrate significant differences in the mean values for the rate of receptor desensitization, whereas Fig. 6*B* (*left* and *right panels*) illustrates more dramatic differences between wild-type and chimeric $P2X_{2b}R$.

The establishment of C-terminal-specific desensitization pattern was also observed in chimeric receptors stimulated with $\alpha\beta$-meATP. Fig. 7*A* shows that wild-type $P2X_2Rs$ do not respond to 10 μM $\alpha\beta$-meATP, whereas chimeric receptors do. Fig. 7*B* illustrates the lack of receptor-specific desensitization

pattern in wild-type $P2X_2Rs$ and a significant difference in the rates of chimeric receptor desensitization in response to 100 μM $\alpha\beta$-meATP. The same conclusions were also derived from cells stimulated with 500 μM $\alpha\beta$-meATP (Fig. 7*C*). Table I summarizes the level of calcium signal desensitization in wild-type and chimeric $P2X_2Rs$. Thus, the introduction of the $P2X_4R$ ectodomain in $P2X_{2a}R$ and $P2X_{2b}R$ backbones had three obvious effects: increase of the rate of receptor desensitization for ATP without affecting the C-terminal-dependent desensitization pattern, reestablishment of the C-terminal-dependent receptor desensitization in response to BzATP and $\alpha\beta$-meATP stimulation, and comparable plateau levels in response to three agonists.

DISCUSSION

In this study, we used the wild-type $P2X_{2a}R$ and $P2X_{2b}R$ because of their identical ectodomains and rapid activation properties, but distinct and well defined desensitization patterns in response to sustained stimulation with ATP (30, 32, 33). The $P2X_4R$ shares about 39% similarity with $P2X_2R$ and desensitizes with rates comparable with those observed in cells expressing $P2X_{2b}R$, whereas $P2X_7R$ shares about 26% similarity with $P2X_2R$ and desensitizes in a manner more comparable with the $P2X_{2a}R$ subtype (6, 34). These four receptors also exhibit highly specific ligand potency profiles, including ATP, BzATP, and $\alpha\beta$-meATP. ATP is a highly potent agonist for $P2X_4R$, a high to middle potency agonist for $P2X_2R$, and a low potency agonist for $P2X_7R$. BzATP is considered as a high potency agonist for $P2X_7R$, a middle potency agonist for $P2X_2R$, and a low potency agonist for $P2X_4R$. $\alpha\beta$-meATP acts as a low potency agonist for $P2X_2R$ and a partial agonist for $P2X_4R$, whereas $P2X_7R$ is insensitive to this agonist (6).

The sequences Ile^{66}–Tyr^{310} of $P2X_2R$, Val^{66}–Tyr^{315} of $P2X_4R$, and Val^{61}–Phe^{313} of $P2X_7R$ used for construction of our chimeric channels contain the majority of residues relevant for ATP binding identified so far. They enclose the 10 conserved cysteine residues among all known P2XRs and three *N*-linked glycosylated sites (Asn^{182}, Asn^{239}, and Asn^{298} in rat $P2X_2R$), which might be responsible for functionality of the channels (35–39). The ectodomain sequences we used also contain several conserved residues, which might contribute to the ATP-binding site, including Lys^{69} and Lys^{71} in rat $P2X_2$ sequence and corresponding to Lys^{68} and Lys^{70} in human $P2X_1$ (9, 10), Trp^{256} in rat $P2X_2$ (40), and Lys^{309} in human $P2X_1$ (9). Because those are common residues for all seven channels, it is obvious that other residues account for ligand specificity among receptors. By exchanging the ectodomain sequences, we hoped that the ligand selectivity profiles would be preserved and thus enabled us to examine the dependence of channel activity on the ligand-binding-specific domains. In accordance with this, our previously published data with $P2X_2 + X_3R$ chimeras having the Val^{60}–Phe^{301} ectodomain sequence of $P2X_3R$ instead of the native Ile^{66}–Tyr^{310} sequence showed highly comparable ligand potency with parental $P2X_3R$ (7, 8).

However, the present data clearly indicate that the transfer of these ectodomains alters the native agonist selectivity and potency. First, the ATP potency for $P2X_{2a} + X_4R$ and $P2X_{2b} + X_4R$ chimeras was higher than that observed in both parental receptors. In parallel to that, two chimeras desensitized more rapidly than parental receptors. Second, $\alpha\beta$-meATP is a partial agonist for $P2X_4R$ (31) and a full and highly potent agonist for $P2X_{2a} + X_4R$ and $P2X_{2b} + X_4R$ chimeras. Third, $P2X_4 + X_2R$ and $P2X_4 + X_7R$ were expressed but were not functioning receptors. These results suggest the effects of transmembrane domain flanking sequences on ligand specificity and agonistic potency. We may speculate that these sequences act as "dominant-positive" and "dominant-negative" domains, depending

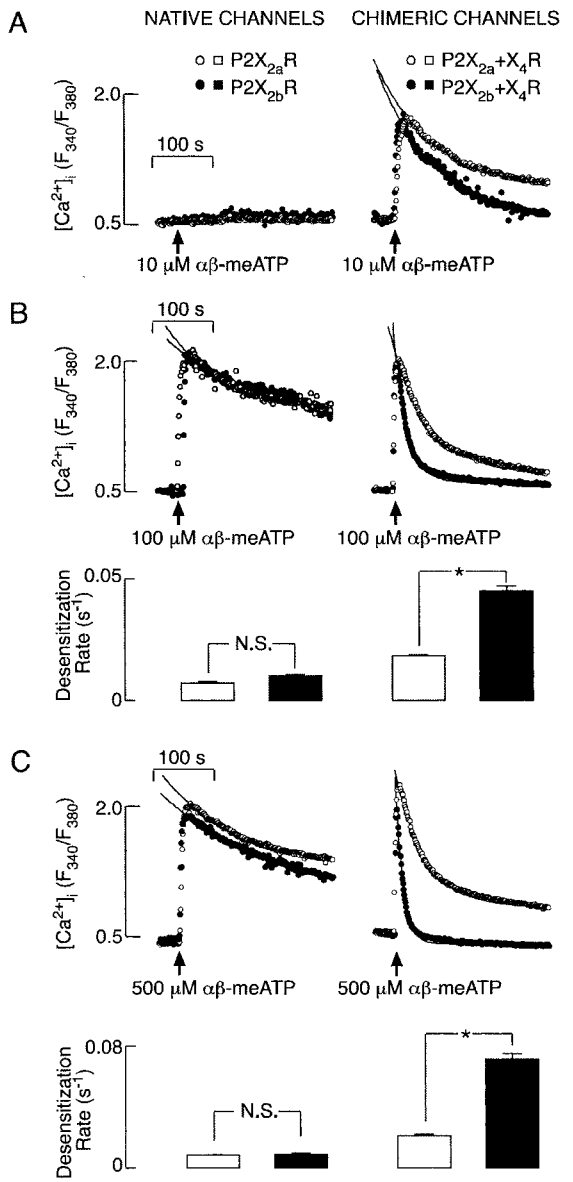

FIG. 7. **Comparison of $\alpha\beta$-meATP-induced calcium responses in cells expressing wild-type (*left panels*) and chimeric (*right panels*) $P2X_2Rs$.** *A*, difference in the sensitivity of wild-type and chimeric channels to 10 μM $\alpha\beta$-meATP. *B* and *C*, comparison of the pattern of calcium signal desensitization in cells expressing wild-type and chimeric receptors during continuous stimulation with 100 μM $\alpha\beta$-meATP (*B*) and 500 μM $\alpha\beta$-meATP (*C*). *Upper panels*, representative traces from 3–8 independent experiments, each done in at least 15 cells. *Bottom panels*, mean values of rates of receptor desensitization.

on the structure of the main ectodomain sequence, to change the sensitivity of receptors for agonists. In accordance with this view, it has been reported recently that point mutations in the first transmembrane domain affect the ligand selectivity of rat $P2X_2R$ (41).

In this study, we also progressed in understanding the mechanism by which the putative ligand-binding domain may influence the rate of receptor desensitization and the relationship between the ectodomain and C-terminal domain in control of desensitization. The main conclusion that emerged from this work is that the P2XR desensitization pattern is receptor- and ligand-specific. The $P2X_{2a}R$-, $P2X_{2b}R$-, and $P2X_4$-specific desensitization patterns were observed in response to ATP, the native agonist for these channels, but were less obvious when stimulated with BzATP and were lost when receptors were stimulated with $\alpha\beta$-meATP. The increase in EC_{50} values for all

three agonists induced by substituting the ectodomains indicated that the potency of agonists reflects the ligand specificity of receptor desensitization, *i.e.* highly potent agonists trigger the subtype-specific desensitization pattern, whereas agonists with lower potency are less effective or are ineffective. Our effort to further establish this hypothesis by generating receptors with decreasing sensitivity for ATP was unsuccessful because $P2X_4 + X_2R$ and $P2X_4 + X_7R$ chimeras were nonfunctional.

On the other hand, we were more successful in establishing that the ectodomain influences desensitization independently of the C-terminal domain. Earlier studies have indicated that the 6-residue receptor-specific sequences in C-terminal influence the rates of $P2X_{2a}R$, $P2X_{2b}R$, $P2X_3R$, and $P2X_4R$ (15). In this study, current and calcium measurements indicated that chimeric $P2X_{2a} + X_4R$ and $P2X_{2b} + X_4R$ desensitized with different rates, *i.e.* a leftward shift in EC_{50} and DC_{50} for chimeric receptors proportionally affected both receptors. This suggests that the C-terminal-dependent desensitization pattern was not affected by substituting the ectodomains. To test this hypothesis further, we generated a mutant of $P2X_{2a} + X_4R$ chimera in which we substituted the C-terminal Arg^{371}–Pro^{376} sequence of $P2X_{2a} + X_4R$ with Glu^{376}–Gly^{381} sequence of $P2X_4R$. In parallel to the desensitization patterns of $P2X_{2a}R$ and $P2X_{2a\text{-}6aa}R$ (15), the present data show that chimeric $P2X_{2a\text{-}6aa} + X_4R$ desensitized more rapidly than $P2X_{2a} + X_4R$ when stimulated with ATP.

At the present time, we cannot speculate about the possible molecular mechanism by which the ligand-binding domain influences receptor desensitization. The main limitation comes from the fact that the ligand-binding domain structure and the crystal structure of P2XRs have not been identified. The structural similarities of P2XRs with class II aminoacyl-tRNA synthases (42) provided a model for initial studies on the ATP-binding domain (9, 10, 40, 41), which could not give a rationale for the receptor behavior shown here. Based on studies with crystallization of glutamate channels, in a recently published study, Sun *et al.* (3) showed that desensitization of these receptors occurs through rearrangement of the dimmer interface, which disengages the agonist-induced conformation change in the binding core from the ion channel gate. To which extent this model provides a rationale for the observed effects with P2XRs is also difficult to discuss, especially with respect to data on the pattern of polymerization of these receptors (43).

The influence of the ectodomain structure on P2XR desensitization is a novel finding for this family of receptors but is reminiscent of those seen among subtypes of other ligand-gated receptor channels. For example, AMPA and glutamate maximally activate AMPA receptors, whereas kainite and domoate act as partial agonists and produce much less desensitization than glutamate (2, 23, 24, 44). A single amino acid mutation in the third loop of the binding pocket of the nicotinic acetylcholine receptor produces a right shift in the concentration-response curve but also significantly slows the rate of channel opening (25). The desensitization of this receptor is affected by amino acids near or within the agonist-binding domain, as well as by residues within M2 that line the pore (26, 27). A single residue substitution in GluR1 also gives a mutant channel that exhibits 6–20-fold lower EC_{50} values for kainate (28). Introduction of the $\alpha 4$ residues in the agonist-binding site of nicotinic nicotinic acetylcholine receptors produces a 100-fold increase in the apparent agonist potency and desensitization of receptors and a 3–7-fold shift in the apparent affinity for activation (27).

In conclusion, our results show that wild-type $P2X_{2a}R$, $P2X_{2b}R$, and $P2X_4R$ desensitized in a receptor- and ligand-specific manner. The $P2X_4R$-specific ligand potency and desensitization patterns were not only transferred but were enhanced in $P2X_{2a} + X_4R$ and $P2X_{2b} + X_4R$, whereas the $P2X_2R$ and $P2X_7R$ ectodomains and the backbone of $P2X_4R$ generated nonfunctional channels. This suggests that flanking sequences around the transmembrane domains may act as modulatory regions. A parallelism in the leftward shift of EC_{50} and DC_{50} for ATP further suggests that the potency of agonists underlines the ligand-specific patterns of receptor desensitization.

REFERENCES

1. Katz, B. & Thesleff, S. (1957) *J. Physiol.* **138,** 63–80
2. Armstrong, N. & Gouaux, E. (2000) *Neuron* **28,** 165–181
3. Sun Y., Olson, R., Horning, M., Armstrong, N., Mayer, M. & Gouaux, E. (2002) *Nature* **417,** 245–253
4. Mayer, M. L., Olson, R. & Gouaux, E. (2001) *J. Mol. Biol.* **311,** 815–836
5. North, R. A. (2002) *Physiol. Rev.* **82,** 1013–1067
6. Khakh, B. S., Burnstock, G., Kennedy, C., King, B. F., North, R. A., Seguela, P., Voigt, M. & Humphrey, P. A. (2001) *Pharmacol. Rev.* **53,** 107–118
7. Koshimizu, T., Ueno, S., Tanoue, A., Yanagihara, N., Stojilkovic, S. S. & Tsujimoto, G. (2002) *J. Biol. Chem.* **277,** 46891–46899
8. He, M.-L., Koshimizu, T., Tomic, M. & Stojilkovic, S. S. (2002) *Mol. Pharmacol.* **62,** 1187–1197
9. Ennion, S., Hagan, S. & Evans, R. J. (2000) *J. Biol. Chem.* **275,** 29361–29367
10. Jiang, L.-H., Rassendren, F., Surprenant, A. & North, R. A. (2000) *J. Biol. Chem.* **275,** 34190–34196
11. Ralevic, V. & Burnstock, G. (1998) *Pharmacol. Rev.* **50,** 413–492
12. North, R. A. & Barnard, E. A. *Curr. Opin. Neurobiol.* **7,** 346–357. 97
13. Lewis, C., Neidhart, S., Holy, C., North, R. A., Buell, G. & Surprenant, A. (1995) *Nature* **377,** 432–435
14. Radford, K. M., Virginio, C., Surprenant, A., North, A. & Kawashima, E. (1997) *J. Neurosci.* **17,** 6529–6533
15. Koshimizu, T., Koshimizu, M. & Stojilkovic, S. S. (1999) *J. Biol. Chem.* **274,** 37651–37657
16. Koshimizu, T., Tomic, M., Koshimizu, M. & Stojilkovic, S. S. (1998) *J. Biol. Chem.* **273,** 12853–12857
17. Smith, F. M., Humphrey, P. P. A. & Murrell-Lagnado, R. D. (1999) *J. Physiol.* **520,** 91–99
18. Surprenant, A., Rassendren, F., Kawashima, E., North, R. A. & Buell, G. (1996) *Science* **272,** 735–738
19. Zhou, Z., Monsma, L. R. & Hume, R. I. (1998) *Biochem. Biophys. Res. Commun.* **252,** 541–545
20. Boue-Grabot, E., Archambault, V. & Seguela, P. (2000) *J. Biol. Chem.* **275,** 10190–10195
21. Ennion, S. J. & Evans, R. J. (2002) *Biochem. Biophys. Res. Commun.* **291,** 611–616
22. Chow, Y.-W. & Wang, H.-L. (1998) *J. Neurochem.* **70,** 2606–2612
23. Patneau, D. K. & Mayer, M. L. (1990) *J. Neurosci.* **10,** 2385–2399
24. Swanson, G. T., Kamboj, S. K. & Cull-Candy, S. G. (1997) *J. Neurosci.* **17,** 58–69
25. Oleary, M. E. & White, M. M. (1992) *J. Biol. Chem.* **267,** 8360–8365
26. Revah, F., Bertrand, D., Galzi, J. L., Devillersthiery, A., Mulle, C., Hussy, N., Berrand, S., Ballivet, M. & Changeux, J. P. (1991) *Nature* **353,** 846–849
27. Corringer, P.-J., Bertrand, S., Bohler, S., Edelstein, S. J., Changeux, J.-P. & Bertrand, D. (1998) *J. Neurosci.* **18,** 648–657
28. Mano, I., Lamed, Y. & Teichberg, V. I. (1996) *J. Biol. Chem.* **271,** 15299–15302
29. Hamill, O. P., Marty, A., Neher, E., Sakmann, B. & Sigworth, F. J. (1981) *Pfluegers Arch. Eur. J. Physiol.* **391,** 85–100
30. Koshimizu, T., Tomic, M., Van Goor, F. & Stojilkovic, S. S. (1998) *Mol. Endocrinol.* **12,** 901–913
31. Jones, C. A., Chessell, I. P., Simon, J., Barnard, E. A., Miller, K. J., Michel, A. D. & Humphrey, P. P. A. (2000) *Br. J. Pharmacol.* **129,** 388–394
32. Brandle, U., Spielmanns, P., Osteroth, R., Sim, J., Surprenant, A., Buell, G., Ruppersberg, J. P., Plinkert, P. K., Zenner, H. P., and Glowatzki, E. (1997) *FEBS Lett.* **404,** 294–298
33. Simon, J., Kidd, E. J., Smith, F. M., Chessell, I. P., Murrell-Lagnado, R., Humphrey, P. P. A. & Barnard, E. A. (1997) *Mol. Pharmacol.* **52,** 237–248
34. Buell, G., Lewis, C., Collo, G., North, R. A. & Surprenant, A. (1996) *EMBO J.* **15,** 55–62
35. Clyne, J. D., Wang, L.-F. & Hume, R. I. (2002) *J. Neurosci.* **22,** 3873–3880
36. Rettinger, J., Aschrafi, A. & Schmalzing, G. (2000) *J. Biol. Chem.* **275,** 33542–33547
37. Hu, B., Senkler, C., Yang, A., Soto, F. & Liang, B. T. (2002) *J. Biol. Chem.* **277,** 15752–15757
38. Ennion, S. J. & Evans, R. J. (2002) *Mol. Pharmacol.* **61,** 303–311
39. Newbolt, A., Stoop, R., Virginio, C., Surprenant, A., North, R. A., Buell, G. & Rassendren, F. (1998) *J. Biol. Chem.* **273,** 15177–15182
40. Nakazawa, K., Ojima, H. & Ohno, Y. (2002) *Neurosci. Lett.* **324,** 141–144
41. Jiang, L.-H., Rassendern, F., Spelta, V., Surprenant, A. & North, R. A. (2001) *J. Biol. Chem.* **276,** 14902–14908
42. Freist, W., Verhey, J. F., Stuhmer, W. & Gauss, D. H. (1998) *FEBS Lett.* **434,** 61–65
43. Nicke, A., Baumert, H. G., Rettinger, J., Eichele, A., Lambrecht, G., Mutschler, E. & Schmalzing, G. (1998) *EMBO J.* **17,** 3016–3028
44. Patneau, D. K., Vyklicky, L. & Mayer, M. L. (1993) *J. Neurosci.* **13,** 3496–3509